KTH ROYAL INSTITUTE
OF TECHNOLOGY

Licentiate Thesis in Civil and Architectural Engineering

On the in-plane mechanical properties of birch plywood

TIANXIANG WANG

Stockholm, Sweden 2022

On the in-plane mechanical properties of birch plywood

TIANXIANG WANG

Academic Dissertation which, with due permission of the KTH Royal Institute of Technology, is submitted for public defence for the Degree of Licentiate of Engineering on Thursday the 15th December 2022, at 10:00 a.m. in M108, Brinellvägen 23, Stockholm.

Licentiate Thesis in Civil and Architectural Engineering
with specialization in Building Materials
KTH Royal Institute of Technology
Stockholm, Sweden 2022

ISBN 978-91-8040-431-0
TRITA-ABE-DLT-2247

Printed by: Universitetsservice US-AB, Sweden 2022

Abstract

Birch plywood has favorable mechanical properties that could be used in new types of connections for timber structures, and thus enable a substitution of the current system with steel plates. Such new connections could result in significant advantages in terms of environmental impact and economy as well as ease of prefabrication and mountability. However, there is a lack of data concerning some of the mechanical properties of birch plywood that would be necessary in order to perform a safe design. In particular, there is a lack of reliable data and understanding of the mechanical properties of birch plywood in directions other than along and perpendicular to the face grain. The aim of this thesis is to gain new knowledge about this anisotropy and to study the variation of the in-plane mechanical properties of birch plywood at different loading angles to the face grain, including effects of size and moisture changes. The goal is that this knowledge will serve as input for the design of birch plywood connections under various loading conditions in timber structures. Specifically, birch plywood specimens were laboratory tested in in-plane tension, compression, shear and bending. The results show that birch plywood possesses the highest tensile, compressive and bending strength and elastic modulus parallel to the face grain and the lowest ones at 45° to the face grain. The opposite findings were noticed for the shear strength and the shear modulus. Moreover, a size effect on the in-plane bending strength property was observed at 0° (parallel) and 90° (perpendicular) to the face grain but not at other angles, which is attributed to the different failure mechanisms. In addition, the increase of moisture leads to the decreased bending strength and elastic modulus in the hygroscopic range. Validated by the experimental work, both analytical and numerical models to predict the mechanical performance of birch plywood under different load conditions and various moisture contents are proposed.

Keywords

Birch plywood, in-plane mechanical properties, load-to-face grain angle, failure criteria, size effect, moisture.

Sammanfattning

Björkplywood har gynnsamma mekaniska egenskaper som skulle kunna användas i nya typer av knutpunkter (förband) för träkonstruktioner, och därmed möjliggöra en substituering av dagens system med stålplåtar. Sådana nya knutpunkter kan innebära avsevärda fördelar när det gäller miljöpåverkan och ekonomi samt en enkel prefabricering och monterbarhet. Det saknas dock data när det gäller vissa mekaniska egenskaper hos björkplywood som är nödvändiga för att kunna utföra en säker design. I synnerhet saknas tillförlitliga data och förståelse kring de mekaniska egenskaperna hos björkplywood i andra riktningar än längs och tvärs dess ytfanér. Syftet med denna avhandling är att ta fram ny kunskap om denna anisotropi och studera variationen av de mekaniska egenskaperna hos björkplywood i dess plan vid olika belastningsvinklar mot ytfanérets fiberriktning, inklusive effekter av storlek och fuktförändringar. Målet är att denna kunskap ska fungera som input för design av björkplywood-förband under olika belastningsförhållanden i träkonstruktioner. Specifikt testades prover av björkplywood i dess plan i drag, tryck, skjuvning och böjning. Resultaten visar att björkplywood har den högsta drag-, tryck- och böjhållfastheten och elasticitetsmodulen parallellt med ytfanérets fiberriktning och den lägsta vid 45° mot densamma. Det motsatta gäller för skjuvhållfasthet och -modul. Dessutom observerades en storlekseffekt avseende böjhållfastheten vid 0° (parallell) och 90° (vinkelrätt) mot ytfanérets fiberriktning men inte vid andra vinklar, vilket förklaras genom de olika brottmekanismerna. Dessutom leder ökningen av fukt till minskad böjhållfasthet och elasticitetsmodul i det hygroskopiska området. Validerat av det experimentella arbetet föreslås både analytiska och numeriska modeller för att förutsäga den mekaniska prestandan hos björkplywood under olika belastningsförhållanden och olika fuktkvoter.

Nyckelord

Björkplywood, mekaniska egenskaper i planet, belastningsvinkel relativt ytfaneren, brott kriterier, storlekseffekt, fukt.

Preface

The work presented in this licentiate thesis was carried out at the Division of Building Materials, Department of Civil and Architectural Engineering, KTH Royal Institute of Technology in Stockholm, Sweden. China Scholarship Council and Svenskt Trä are gratefully acknowledged for the financial support. The work has also been supported by the Vinnova project 2017-02712 “Bärande utomhusträ” within the BioInnovation program as well as the Kamprad Family Foundation (reference number: 20200013) and from Produktion2030, a strategic innovation program supported by Vinnova [reference number: 2021-03681], Swedish Energy Agency, Formas including the industry partners.

Firstly, I would like to express my gratitude to my supervisors Prof. Roberto Crocetti and Prof. Magnus Wålinder for taking me on board since the master program, for the valuable guidance, advice and encouragement.

Special thanks to my colleague, co-author and friend Yue Wang. The work would not be complete without your contribution, the thoughts and discussions shared between us.

Koskisen is acknowledged for supplying birch plywood materials. Moelven is thanked for the technical communication. Viktor Brolund, Gürsel Hakan Taylan and Hassan Abdulazim Fadil Mohammed are sincerely thanked for their technical support during the laboratory tests.

Finally, I would like to thank my family and friends, and most importantly, my wife Chui Ping Lai for their endless support, especially during the pandemic period.

Stockholm, October 2022
Tianxiang Wang

List of appended papers

This thesis is based upon the following scientific articles referred to in the text by their roman numbers:

Paper I

Wang, T., Wang, Y., Crocetti, R., Wålinder, M. (2022) In-plane mechanical properties of birch plywood. Construction and Building Materials, 340, 127852.

Paper II

Wang, T., Wang, Y., Crocetti, R., Wålinder, M. (2022) Influence of face grain angle, size, and moisture content on the edgewise bending strength and stiffness of birch plywood. Materials & Design, 223, 111227.

In the appended papers, the first author planned and performed the majority of the experiments, analyzed the analytical and numerical models, wrote the manuscript with the help of the co-authors.

Nomenclature

Abbreviations

COV	Coefficient of Variation
EWP	Engineered wood product
LVDT	Linear variable differential transformer
MC	Moisture content
RH	Relative humidity
RMSE	Root mean square error
T	Temperature

Latin Symbols

A	Cross-sectional area	[m²]
A_1	Ratio between E_y and E_x	[1]
b	Width of birch plywood	[m]
d	Depth of birch plywood	[m]
$E_{t(c)}$	Tensile or compressive elastic modulus	[N m⁻²]
E_x	On-axis elastic modulus in x direction	[N m⁻²]
E_y	On-axis elastic modulus in y direction	[N m⁻²]
E_z	On-axis elastic modulus in z direction	[N m⁻²]
E_θ	Elastic modulus at θ to the face grain	[N m⁻²]
f_b	Edgewise bending strength	[N m⁻²]
f_t	Tensile strength	[N m⁻²]
f_x	On-axis normal strength	[N m⁻²]
f_{xc}	On-axis normal strength in compression	[N m⁻²]
f_{xt}	On-axis normal strength in tension	[N m⁻²]
f_{xy}	On-axis shear strength	[N m⁻²]
f_y	On-axis normal strength	[N m⁻²]
f_{yc}	On-axis normal strength in compression	[N m⁻²]
f_{yt}	On-axis normal strength in tension	[N m⁻²]
$f_{\theta,exp}$	Experimental strength at θ to the face grain	[N m⁻²]
$f_{\theta,pre}$	Predicted strength at θ to the face grain	[N m⁻²]
F_{12}	Interaction coefficient	[N⁻² m⁴]
F_c	Resultant force in the compressive zone	[N]
F_{max}	The failure load	[N]
F_t	Resultant force in the tensile zone	[N]
ΔF	Load increment	[N]
$G_{destructive}$	Shear modulus from destructive tests	[N m⁻²]

$G_{modified}$	Modified shear modulus	[N m^{-2}]
G_{xy}	On-axis shear modulus in x-y plane	[N m^{-2}]
G_{xz}	On-axis shear modulus in x-z plane	[N m^{-2}]
G_{yz}	On-axis shear modulus in y-z plane	[N m^{-2}]
G_{θ}	Shear modulus at θ to the face grain	[N m^{-2}]
I	Second moment of area	[m^4]
k	Shear correction coefficient	[1]
l_1	Original length of strain gauge	[m]
l_r	Reduced length	[m]
L	Span of birch plywood	[m]
m	Cosine function of an angle θ	[1]
$M_{u,anl}$	Analytical ultimate moment capacity	[N m]
$M_{u,exp}$	Experimental ultimate moment capacity	[N m]
$M_{u,num}$	Numerical ultimate moment capacity	[N m]
MOE_b	Elastic bending modulus	[N m^{-2}]
n	Sine function of an angle θ	[1]
t	Thickness of birch plywood	[m]
t_1	Thickness of inner veneer	[m]
t_2	Thickness of face veneer	[m]
Δu	Deformation increment	[m]
Δu_b	Bending deformation increment	[m]
Δu_{LVDT}	LVDT deformation increment	[m]
Δu_s	Shear deformation increment	[m]
W	Elastic section modulus	[m^3]
y_t	Depth of the tensile zone	[m]
y_c	Depth of the compressive zone	[m]
z	Lever arm	[m]

Greek Symbols

γ	Shear strain	[1]
$\gamma_{correction}$	Correction factor	[1]
$\varepsilon_{t(c)}$	Tensile or compressive strain	[1]
ε_{tu}	Tensile strain at failure	[1]
θ	Face grain angle to the loading or beam axis	[°]
ν_{xy}	Poisson's ratio in x-y plane	[1]
ν_{xz}	Poisson's ratio in x-z plane	[1]
ν_{yz}	Poisson's ratio in y-z plane	[1]
σ_1	Off-axis normal stress in the 1-2 system	[N m^{-2}]
σ_2	Off-axis normal stress in the 1-2 system	[N m^{-2}]
$\sigma_{t(c)}$	Tensile or compressive stress	[N m^{-2}]
σ_x	On-axis normal stress in the x-y system	[N m^{-2}]

σ_y	On-axis normal stress in the x-y system	[N m^{-2}]
τ	Shear stress	[N m^{-2}]
τ_{12}	Off-axis shear stress in the 1-2 system	[N m^{-2}]
τ_{xy}	On-axis shear stress in the x-y system	[N m^{-2}]

Contents

1. Introduction

1.1. Plywood

Plywood is one of the earliest produced engineered wood products (EWPs). It is composed of an uneven number of thin veneers (also called plies), normally with a thickness from less than one millimeter to several millimeters, bonded together with an adhesive and with the grain direction of adjacent veneers perpendicular to one another [1]. See Figure 1 for the cross-lamination configuration.

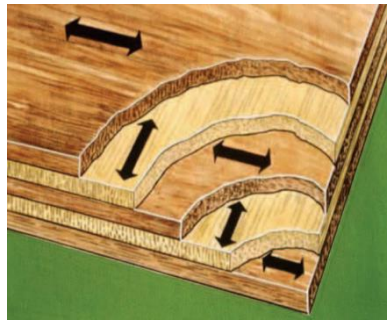

Figure 1: The cross-lamination in plywood [2].

The manufacturing processes of plywood comprise conditioning (usually by heating of the stem in a water bath), peeling, drying, grading, lay-up, bonding, pre-pressing, hot pressing and finishing. These basic steps are similar in most parts of the world. However, some minor differences regarding the manufacturing details might exist depending on the different physical and chemical properties of the wood raw material, the application fields of plywood products and the regions where the mills are located [2-4].

The important features of plywood compared to sawn timber are the improved dimensional stability, the possibility to overcome the dimensional limitation caused by the normal size of the trees and the redistributed natural defects, etc. [5, 6].

In terms of the mechanical properties, it is well-known that timber is an anisotropic material, with high strength and stiffness in the longitudinal direction but much lower values in the radial and tangential directions. Plywood, on the other hand, due to the cross-lamination configuration, shows values of strength and stiffness much more balanced in different directions of the plane.

Regarding the number of veneers, the commonly produced plywood has at least 3 veneers to up to 35 veneers [7]. It is straightforward that the increased number of veneers leads to a lower degree of anisotropy provided that the veneer thickness is constant [8]. The configuration of plywood also enhances its resistance to splitting because there is no line of cleavage; thus fasteners can be inserted at closer spacing or nearer to the edges than in unidirectional timber products [9].

1.2. Structural applications of plywood

Due to the aforementioned advantages, plywood exhibits versatile applications for structural purposes. Strength, stiffness and the durability of the wood-adhesive bond are important for structural plywood while the appearance of the face veneer may or may not be of significance. Typical structural applications of plywood are listed below [1, 10, 11]:

- building construction systems, e.g., sub-flooring, decking, sheathing, bracing, roof, shear wall, concrete formwork, etc.;
- connection systems, e.g., gusset plates in truss system, beam-to-beam connection, beam-to-column connection, etc.;
- beam systems, e.g., webs in I-beam or box beam systems;
- aircraft.

Among these applications, connections are of the most interest in this thesis. Plywood can be applied as the gusset plates in truss systems, where the axial forces in different directions are transferred. Plywood plates could

also be utilized in moment-resisting connections, e.g., beam-to-beam, beam-to-column and portal frame haunches, etc., where a bending moment is induced as well. See Figure 2 for the illustration of plywood applications in timber connections [12, 13].

Figure 2: Illustration of plywood applications in timber connections [12, 13].

However, in high-rise timber buildings as well as long-span timber applications, slotted-in steel plates are dominant [14]. For instance, the 14-story timber building 'Treet', located in Bergen, Norway, is one of the tallest timber buildings worldwide with a height of around 49 m. All glulam elements in this building are connected by using 8 mm slotted-in steel plates and 12 mm dowels [15]. Comprehensive analyses of timber connections with slotted-in steel plates have been carried out during the past few decades [16-18]. The failure model of the slotted-in steel plates is better developed than that of the plywood gusset plates and previous research on plywood gusset plates is not sufficient.

Plywood plates, compared to the slotted-in steel plates, are more environmentally friendly, cost-effective and less prefabrication demanding. In addition, plywood plates have better workability and higher tolerance during assembly, with better fire resistance. Thus, it is worth considering plywood as a promising alternative to steel plates in timber connections.

More attention has been raised recently to plywood made of birch (Betula pendula) [19, 20]. Birch has a wide natural distribution area in Europe and Asia, especially in the Nordic and Baltic countries [21]. Some physical and mechanical properties of common species in Scandinavia are listed in Table 1 [22, 23]. It is indicated that, as a type of hardwood, birch possesses outstanding mechanical properties compared to softwood species.

Table 1: Some physical and mechanical properties of common species in Scandinavia [22, 23].

Species		Density (dry) (kg/m^3)	Tensile strength in fiber direction (MPa)	Compressive strength in fiber direction (MPa)	Elastic modulus in fiber direction (MPa)
Soft wood	Pine (Pinus silvestris)	450-500	102	45-47	10000-12000
	Spruce (Picea abies)	370-440	88	35-44	8300-13000
	Larch (Larix decidua)	520-600	105	47-54	9900-13500
Hard wood	**Birch (Betula pendula)**	**580-620**	**137**	**54-60**	**13000-15000**
	Oak (Quercus robur)	650-720	90	53-65	10000-13000
	Beech (Fagus sylvatica)	640-680	135	52-56	10000-16000

Note: The values for the strength and elastic properties are the mean values determined from the clear wood at 12% moisture content (MC).

1.3. Aim and objectives

The aim of this thesis is to gain new knowledge about the in-plane mechanical properties of birch plywood at various loading angles to the face grain. Specifically, the in-plane tensile, compressive, shear and bending strength and elastic properties have been studied. In-plane

bending is also referred to as edgewise bending. Out-of-plane (flatwise) bending is not within the scope since it is barely activated when using birch plywood as gusset plates. The characterization of the in-plane mechanical properties is vital as it is the first step in the design of a birch plywood gusset plate.

Some researchers have studied the mechanical properties of plywood under different angles between the face grain and the load direction [24-27]. However, the investigations relates to other species than birch. Birch plywood is rarely used in structural engineering applications and only the mechanical properties parallel and perpendicular to the face grain can be found in the literature [7].

The first objective of this thesis is to establish a comprehensive experimental database of the in-plane tensile, compressive, shear and bending strength and stiffness at a few loading angles to the face grain between 0° and 90°.

The second objective of this thesis is to predict the aforementioned properties at any angle to the face grain by means of analytical and numerical models.

The size of plywood plates as well as the surrounding environmental conditions (temperature (T) and relative humidity (RH)) in practical structural applications are in general different from those encountered during laboratory testing. Therefore, the third objective of this thesis is to study the influence of both size and moisture content on the edgewise bending strength and stiffness of birch plywood.

1.4. Thesis structure

This thesis begins with a first introductory chapter, in which the background, motivation, aim and objectives are presented. Chapter 2 contains a description of the investigated material and methods. Chapter 3 presents and discusses the experimental and prediction results of the in-plane tensile, compressive, shear and bending strength and elastic properties. Finally, Chapter 4 concludes the main findings in this thesis and suggests future work to be performed.

2. Materials and methods

2.1. Materials

The studied birch plywood is composed of 15 veneers with the nominal thickness of 21 mm. The veneer layup can be notated as $[0,(0, 90)_6,(0)_2]$. The inner 13 veneers have an identical thickness of 1.4-1.5 mm while the face veneers are thinner since the surfaces of the plywood were sanded in the production line for the control of the total thickness. The veneer layup of birch plywood is illustrated in Figure 3. The ratio between the thickness of the veneers, parallel and perpendicular to the face grain direction, respectively, is approximately 4:3. Phenol formaldehyde resin was used as adhesive between each veneer. All the birch plywood specimens were cut from six 1500 mm-by-3000 mm plywood panels. These panels were produced by Koskisen Oy (Järvelä, Finland). Given that the birch plywood panels are commercial products, details of the manufacturing processes, including the pressing schedule and the characteristics of the phenol formaldehyde resin, etc., are not described in the thesis.

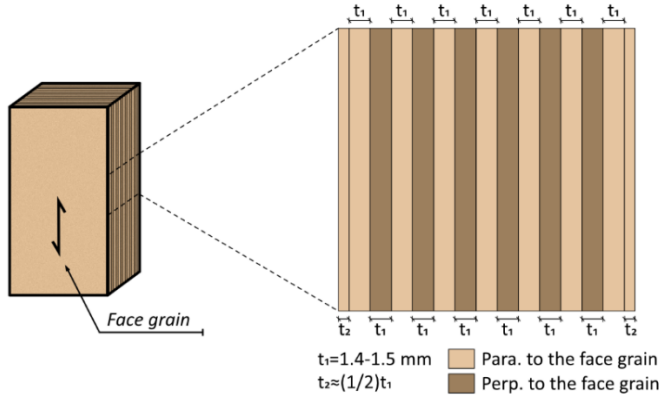

Figure 3: The veneer layup of birch plywood specimen.

2.2. In-plane tensile, compressive and shear properties

2.2.1. Experiments

For each type of test (tension, compression and shear), birch plywood specimens were tested at five load-to-face grain angles, from 0° (parallel) to 90° (perpendicular), with an interval of 22.5°. Each test series had 12 repetitions, resulting in 180 specimens in total. Prior to the tests, the specimens were conditioned in a climate chamber (T= 20 °C, RH= 65%) until the mass did not change more than 0.1% at an interval of six hours. Density was then measured on compressive specimens as they have the regular shape, thus the volume can be easily determined. MC was evaluated on 12 additional replicates with similar mass to the tested specimens based on the oven-dry method [28]. The mean density and MC were approx. 693 kg/m^3 and 12%, respectively.

The test setup and the configuration of birch plywood specimens were adapted from the testing standard ASTM D3500 [29] for tensile tests, ASTM D3501 [30] for compressive tests and EN 789, ASTM D1037, ASTM D2719 [31-33] for the shear tests. Two 38 mm-long strain gauges were installed for the measurement of the elastic properties. Details regarding the test procedure have been introduced in Paper I. See Figure 4 for the test setup and the information about the specimens.

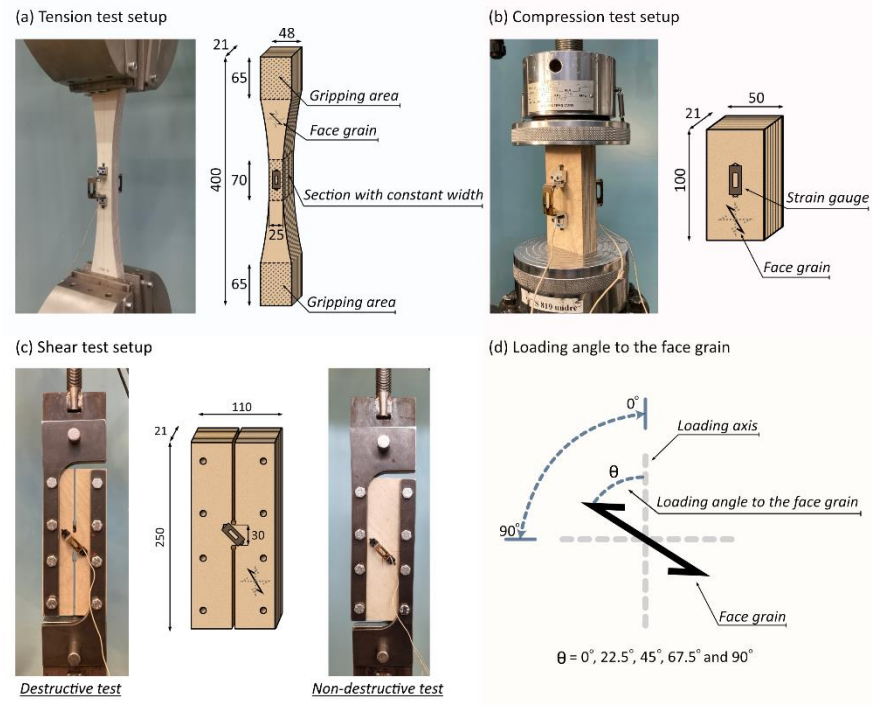

Figure 4: Test setup: (a) tension, (b) compression and (c) shear. (d) Illustration of the loading angle to the face grain (unit of dimension: mm).

It is noticed in Figure 4b that there is one spherical seat platen connected to the loading head. This is to ensure the full contact with the top surface of the specimen during compressive loading.

Tensile and compressive strengths are defined as the failure load applied divided by the cross-sectional area. The tensile and compressive elastic modulus are determined as the slope of the linear portion of the stress-strain curve, as expressed in Eq. 1.

$$E_{t(c)} = \frac{\sigma_{t(c)}}{\varepsilon_{t(c)}} = \frac{\Delta F/A}{\Delta u/l_1}, \qquad (1)$$

where $E_{t(c)}$ is the tensile or compressive elastic modulus; $\sigma_{t(c)}$ is the tensile or compressive stress; $\varepsilon_{t(c)}$ is the tensile or compressive strain; ΔF is the increment of the load between 15% to 35% of the failure load; Δu is the increment of deformation measured from the strain gauges corresponding

to ΔF; l_1 is the original length of strain gauge; and A is the cross-sectional area. The chosen range, i.e., 15-35%, fulfills the requirement in ASTM D3501 [30] that at least 20% of the ultimate load is covered.

As shown in Figure 4c, the configuration of the shear specimen in the destructive test was designed with a reduced length in the middle to lower the capacity. The shear strength can be well characterized by the destructive tests and is defined as the failure load divided by the cross-sectional area between the vertical slots. However, the shear modulus determined from the destructive tests should be modified by a correction factor based on the non-destructive test results. This is due to that, in the destructive tests, shear deformation was concentrated along the middle line but the strain gauges measured the average deformation between the attached points (38 mm long), resulting in the overestimation of the shear modulus. In contrast, the shear strain in the non-destructive test was nearly uniform within the area where the strain gauges were attached. Therefore, non-destructive tests were performed on specimens without slits at 0°, 45° and 90°, with 5 replicates for each angle.

The shear modulus obtained from the destructive tests is expressed in Eq. 2.

$$G_{destructive} = \frac{\tau}{\gamma} = \frac{\Delta F/(l_r \cdot t)}{2\Delta u \cdot / l_1}, \quad (2)$$

where $G_{destructive}$ is the shear modulus derived from the destructive tests; τ is the shear stress; γ is the shear strain; ΔF is the increment of the load between 15% and 35% of the failure load; l_r is the reduced length in the middle; t is the thickness of the specimen; Δu is the increment of deformation measured from the strain gauges corresponding to ΔF; and l_1 is the length of the strain gauge.

The modified shear modulus is shown in Eq. 3.

$$G_{modified} = \gamma_{correction} \cdot G_{destructive}, \quad (3)$$

where $G_{modified}$ is the modified shear modulus; and $\gamma_{correction}$ is the correction factor, which is the ratio of the shear modulus measured from the specimens without slits (non-destructive tests) and with slits

(destructive tests). This ratio is determined to be 0.33, 0.35 and 0.32, at 0◦, 45◦ and 90◦ to the face grain, respectively, leading to the mean correction factor ($\gamma_{correction}$) of 0.33. It is noted that the shear modulus results presented in the chapters below are the modified ones ($G_{modified}$).

2.2.2. Predictions of off-axis strength

In order to predict the off-axis strength in tension, compression and shear, the first step was to transform the uniaxial stress in the 1-2 (parallel–perpendicular to the loading axis) coordinate system to the x-y (parallel–perpendicular to the face grain of the birch plywood) coordinate system. The transformation equation between the off-axis stresses and the on-axis stresses is shown in Eq. 4.

$$\begin{bmatrix}\sigma_x\\ \sigma_y\\ \tau_{xy}\end{bmatrix} = \begin{bmatrix} m^2 & n^2 & 2mn \\ n^2 & m^2 & -2mn \\ -mn & mn & m^2-n^2\end{bmatrix}\begin{bmatrix}\sigma_1\\ \sigma_2\\ \tau_{12}\end{bmatrix}, \quad (4)$$

where $m = \cos(\theta)$; $n = \sin(\theta)$; θ is the angle between the load direction and the face grain; σ_1, σ_2 and τ_{12} are the off-axis stresses in the 1-2 system; and σ_x, σ_y and τ_{xy} are the on-axis stresses in the x-y system. σ_1, σ_2, σ_x and σ_y are defined as positive in tension and negative in compression while τ_{12} and τ_{xy} are positive with the direction shown in Figure 5b and 5c. There is only σ_1 ($\sigma_2 = \tau_{12} = 0$) in tensile and compressive tests and only τ_{12} ($\sigma_1 = \sigma_2 = 0$) in panel shear tests.

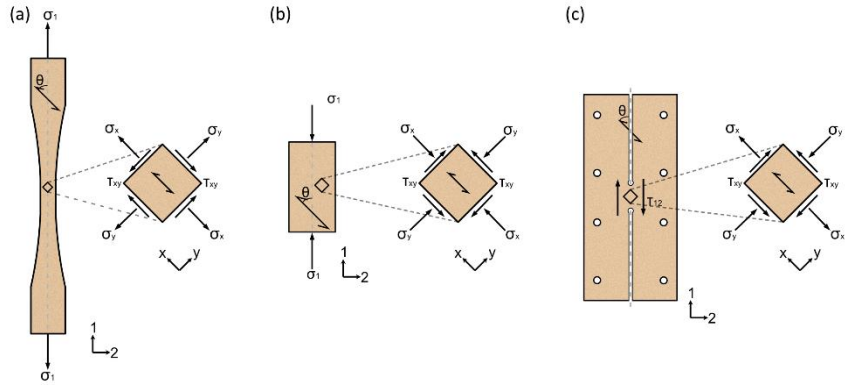

Figure 5: Stress transformation of the (a) tensile, (b) compressive and (c) shear specimens.

After transforming the stresses from 1-2 to x-y coordinate system, the second step was to employ a number of failure criteria to predict the off-axis strength based on the on-axis strength values. Several failure criteria (listed in Table 2) that are widely used for composite materials were examined in this thesis for their applicability to birch plywood.

Table 2: Failure criteria for off-axis strength predictions.

Failure criteria	Formula	Eq.
Hankinson [34]	$\frac{\sigma_x}{f_x}+\frac{\sigma_y}{f_y}=1$	(5)
Linear criterion with shear effect	$\left\|\frac{\sigma_x}{f_x}\right\|+\left\|\frac{\sigma_y}{f_y}\right\|+\left\|\frac{\tau_{xy}}{f_{xy}}\right\|=1$	(6)
Empirical Norris [35]	$\left(\frac{\sigma_x}{f_x}\right)^2+\left(\frac{\sigma_y}{f_y}\right)^2+\left(\frac{\tau_{xy}}{f_{xy}}\right)^2=1$	(7)
Theoretical Norris [35]	$\left(\frac{\sigma_x}{f_x}\right)^2-\frac{\sigma_x\sigma_y}{f_xf_y}+\left(\frac{\sigma_y}{f_y}\right)^2+\left(\frac{\tau_{xy}}{f_{xy}}\right)^2=1$ $or\ \left(\frac{\sigma_x}{f_x}\right)^2=1\ or\ \left(\frac{\sigma_y}{f_y}\right)^2=1$	(8)
Tsai-Hill [36, 37]	$\left(\frac{\sigma_x}{f_x}\right)^2-\frac{\sigma_x\sigma_y}{{f_x}^2}+\left(\frac{\sigma_y}{f_y}\right)^2+\left(\frac{\tau_{xy}}{f_{xy}}\right)^2=1$	(9)
Hoffman [38]	$\frac{{\sigma_x}^2-\sigma_x\sigma_y}{f_{xc}f_{xt}}+\frac{{\sigma_y}^2}{f_{yc}f_{yt}}+\frac{f_{xc}-f_{xt}}{f_{xc}f_{xt}}\sigma_x+\frac{f_{yc}-f_{yt}}{f_{yc}f_{yt}}\sigma_y+\left(\frac{\tau_{xy}}{f_{xy}}\right)^2=1$	(10)
Tsai-Wu [39]	$\frac{{\sigma_x}^2}{f_{xc}f_{xt}}+\frac{{\sigma_y}^2}{f_{yc}f_{yt}}+2F_{12}\sigma_x\sigma_y+\frac{f_{xc}-f_{xt}}{f_{xc}f_{xt}}\sigma_x+\frac{f_{yc}-f_{yt}}{f_{yc}f_{yt}}\sigma_y+\left(\frac{\tau_{xy}}{f_{xy}}\right)^2=1$	(11)

f_x, f_y and f_{xy} are the on-axis normal and shear strengths of birch plywood. The mean values obtained from the experiments are used as input for these strength properties. It is worth noting that the first two failure criteria, namely, Hankinson and linear criteria with shear effect are only capable for the prediction of the off-axis tensile and compressive strengths but not

the shear strengths because the Hankinson's criterion neglects the shear contribution and, for the linear criterion with shear effect, the shear term is only in the first order. Hoffman and Tsai-Wu failure criteria distinguish the on-axis normal strengths in tension and compression, which are specified by f_{xt}, f_{xc}, f_{yt} and f_{yc}. In addition, the interaction coefficient F_{12} in Tsai-Wu failure criterion is unknown due to the complexity of experimentally determining this value. However, F_{12} is constrained by certain stability conditions. See the inequality in Eq. 12.

$$-\sqrt{\frac{1}{f_{xc}f_{xt}f_{yc}f_{yt}}} \leq F_{12} \leq \sqrt{\frac{1}{f_{xc}f_{xt}f_{yc}f_{yt}}}, \tag{12}$$

F_{12} was first assumed as zero to compare with the experimental data and other failure criteria. Hereafter, the influence of this parameter on the predicted strength was studied by varying F_{12} from its lower limit to the upper limit.

2.2.3. Predictions of off-axis elastic properties

Both elastic modulus and shear modulus were predicted. Three models were applied for elastic modulus predictions (see Table 3) and two models were applied for shear modulus predictions (see Table 4).

Table 3: Off-axis elastic modulus prediction models.

Elastic modulus prediction models	Formula	Eq.
Hankinson	$E_\theta = \frac{E_x \cdot E_y}{E_y \cdot cos^2(\theta) + E_x \cdot sin^2(\theta)}$	(13)
Transformation model (elastic modulus) [40, 41]	$\frac{1}{E_\theta} = \frac{1}{E_x} cos^4(\theta) + \left(-2\frac{\nu_{xy}}{E_x} + \frac{1}{G_{xy}}\right) cos^2(\theta) sin^2(\theta) + \frac{1}{E_y} sin^4(\theta)$	(14)
Saliklis and Falk [42]	$\frac{1}{E_\theta} = \frac{1}{E_x} cos^4(\theta) + \left(\frac{1}{{A_1}^{2A_1} G_{xy}}\right) cos^2(\theta) sin^2(\theta) + \frac{1}{E_y} sin^4(\theta)$	(15)

Table 4: Off-axis shear modulus prediction models.

Shear modulus prediction models	Formula	Eq.
Transformation model (shear modulus)	$\frac{1}{G_\theta} = 4(\frac{1}{E_x} + \frac{1}{E_y} - 2\frac{-\nu_{xy}}{E_x}) cos^2(\theta) sin^2(\theta) + \frac{1}{G_{xy}} (cos^2(\theta) - sin^2(\theta))^2$	(16)
Modified transformation model (shear modulus)	$G_\theta = \frac{G_{xy} \cdot G_{45}}{G_{xy} \cdot sin^2(2\theta) + G_{45} \cdot cos^2(2\theta)}$	(17)

E_θ and G_θ are the off-axis elastic and shear modulus at an angle θ to the face grain; E_x and E_y are the elastic modulus parallel and perpendicular to the face grain determined from the tensile tests; G_{xy} is the on-axis shear modulus determined from the shear tests; ν_{xy} is the Poisson's ratio in x-y

plane derived based on the mechanical properties of solid birch and the cross-sectional configuration of the plywood [8, 43]; and the parameter A_1 in Eq. 15 is the ratio between E_y and E_x.

2.3. Edgewise bending properties

2.3.1. Experiments

The influence of three factors, i.e., face grain angle, size and moisture content, on the edgewise bending properties was investigated by testing 288 birch plywood specimens (24 test series with 12 repetitions) in three-point bending.

The test setup is shown in Figure 6.

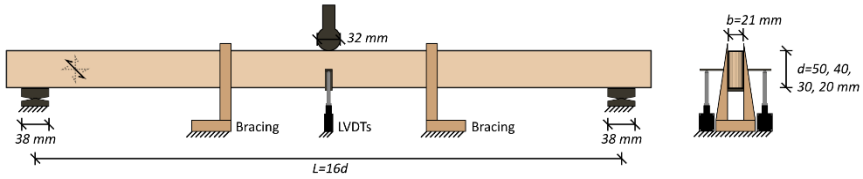

Figure 6: Sketch of the test setup.

The birch plywood specimens tested in edgewise bending have the same veneer layup as the ones tested in tension, compression and shear, with the nominal width (b) of 21 mm. The depth (d) varies from 50 mm to 20 mm with an interval of 10 mm to study the size effect; thus, the span (L)–to-depth ratio is kept constant as 16 in all the tests. It is noted that the bracings were only used in the beams with the nominal depth of 50 mm to minimize the lateral instability during the loading. The beams with smaller sizes were not necessary to be laterally braced. The information with regards to the test series is summarized in Table 5.

Table 5: Information regarding the test series

Test series No.	MC (%)	*d* (nominal) (mm)	Angle (°)	*d* (actual) (mm)	*b* (actual) (mm)	Density (kg/m^3)
01	11.9	50	0	49.95 (0.3%)	20.55 (0.3%)	703.4 (1.8%)
02			22.5			
03			45			
04			67.5			
05			90			
06	11.9	40	0	39.93 (0.2%)	20.61 (0.6%)	700.7 (1.8%)
07			90			
08	11.9	30	0	30.30 (0.4%)	20.53 (0.3%)	704.9 (1.7%)
09			90			
10*	11.9	20	0	20.29 (1.3%)	20.57 (0.2%)	700.4 (1.9%)
11*			22.5			
12*			45			
13			67.5			
14			90			
15	7.2	20	0	20.24 (1.3%)	20.23 (0.3%)	687.7 (2.1%)
16			22.5			
17			45			
18			67.5			
19			90			
20	21.8	20	0	20.37 (1.1%)	21.21 (0.7%)	728.1 (2.0%)
21			22.5			
22			45			
23			67.5			
24			90			

Note: the experimental results of the test series No.10-12 with asterisks have been reported in [44]. In the columns '*d* (actual)', '*b* (actual)' and 'Density', the numbers within parentheses indicate the Coefficient of Variation (COV).

Three properties were determined from the tests, i.e., ultimate moment capacity, bending strength and elastic bending modulus. The experimental

ultimate moment capacity is defined as the maximum bending moment at mid-span (see Eq. 18).

$$M_{u,exp} = \frac{F_{max} \cdot L}{4}, \tag{18}$$

where $M_{u,exp}$ is the experimental ultimate moment capacity; F_{max} is the failure load. The edgewise bending strength (f_b) is defined as $M_{u,exp}$ over the elastic section modulus W. The elastic bending deformation is calculated from the linear portion of the load-displacement curves (Eq. 19).

$$MOE_b = \frac{\Delta F \cdot L^3}{48 \cdot I \cdot \Delta u_b} = \frac{\Delta F \cdot L^3}{4 \cdot b \cdot d^3 \cdot (\Delta u_{LVDT} - \Delta u_s)}, \tag{19}$$

where MOE_b is the elastic bending modulus; ΔF is the force increment between 15% to 35% of the failure load; I is the second moment of area; Δu_b is the increment of the bending deformation at mid-span corresponding to ΔF; Δu_{LVDT} is the average displacement increment measured from two linear variable differential transformers (LVDTs) corresponding to ΔF; and Δu_s is the increment of shear deformation at mid-span corresponding to ΔF (see Eq. 20).

$$\Delta u_s = \frac{\Delta F \cdot L}{4 \cdot k \cdot G_\theta \cdot A}, \tag{20}$$

where k is the shear correction coefficient. k is assumed to be 5/6, for orthotropic laminate materials [45]. G_θ is the mean experimental shear modulus at an angle θ to the face grain. The local bearing deformation at the supports is negligible for birch plywood due to the cross lamination configuration.

2.3.2. Prediction models

It is also of interest to develop the prediction models to predict the angle-dependency of the edgewise bending properties, as the prediction model, once validated, could provide key information for the structural design of birch plywood gusset plates. There is no doubt that, when birch plywood beams are loaded in edgewise positive bending, the upper part is subjected to compressive stresses while the lower part is in tension. Thus, the stress-

strain relationships in uniaxial tension and compression are required as the input in the prediction model, which are obtained from the tensile and compressive tests in this study.

2.3.2.1. Analytical model

In the analytical prediction model, the strain and stress distributions along the depth of the birch plywood beam at mid-span could be derived based on the force equilibrium in the compressive and tensile zone. See Figure 7 for the schematic representation of strain and stress distributions at the ultimate failure state. Failure is defined when the maximum tensile stress at the bottom of the beam reaches the tensile strength f_t.

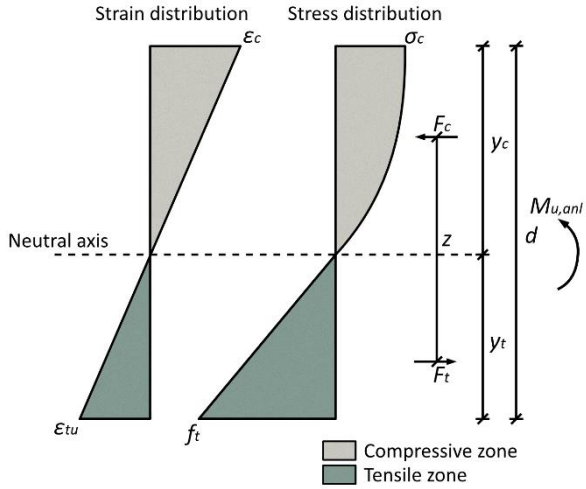

Figure 7: Strain and stress distributions along the depth at mid-span when the maximum tensile stress reaches the tensile strength.

The relationships between the tensile and compressive zones are illustrated in Eq. 21 and 22.

$$\frac{y_t}{y_c} = \frac{\varepsilon_{tu}}{\varepsilon_c}, \tag{21}$$

$$y_t + y_c = d, \tag{22}$$

where y_t and y_c are the depth of the tensile and compressive zones respectively; ε_{tu} is the tensile strain at failure; and ε_c is the compressive strain at the top of the beam when the failure occurs. The unknowns, i.e., y_t, y_c, ε_c, σ_c, F_t, F_c and z, can be calculated based on the force equilibrium in the compressive and tensile zone (see Eq. 23).

$$\sum F_i = F_t - F_c = 0, \tag{23}$$

where F_t and F_c are the resultant forces in the tensile and compressive zones; σ_c is the compressive stress at the top of the beam when the failure occurs; z is the lever arm between the resultant forces. The analytical ultimate moment capacity $M_{u,anl}$ is therefore calculated in Eq. 24.

$$M_{u,anl} = F_{t(c)} \cdot z, \tag{24}$$

2.3.2.2. Numerical model

3D solid models were created via the commercial FEM package Abaqus/Standard (Simulia, USA). In the numerical model, apart from the compressive elasto-plastic stress-strain relationships, some engineering constants should also be provided, as listed in Table 6. They consist of the density ρ, elastic modulus E_{i}, the Poisson's ratio ν_{ij} and the shear modulus G_{ij}. The subscripts (i, j = x, y, z) stand for the principal material directions.

Table 6: Engineering constants of birch plywood for numerical analysis

ρ (kg/m³)	E_{x} (MPa)	E_{y} (MPa)	E_{z} (MPa)	ν_{xy}
703.4	9400	6700	1110	0.036
ν_{xz}	ν_{yz}	G_{xy} (MPa)	G_{xz} (MPa)	G_{yz} (MPa)
0.443	0.427	600	206	186

Note: ρ is the mean density of the specimens from test series No. 01-05. E_{x}, E_{y} and G_{xy} are the mean values presented in Figure 9 (tensile tests) and Figure 10 in Section 3.1.1. The rest of the engineering constants were derived or found in the literature [7, 8, 43], which have been explained in detail in Paper II.

The on-axis stresses in the bottom line of the model at mid-span were checked. Failure is defined when the empirical Norris failure criterion is reached. The reason to employ this failure criterion is explained in Section 3.1.2. The numerical ultimate moment capacity is referred to $M_{u,num}$. The mesh element type was chosen to be the 8-node hexahedral brick element with reduced integration (C3D8R in ABAQUS/CAE 6.14). The mesh size was 2.5 mm.

3. Results and discussion

3.1. In-plane tensile, compressive and shear properties

3.1.1. Experimental results

All the stress-strain curves at five different angles in tension, compression and shear are plotted in Figure 8 until reaching the failure load. The typical curves, i.e., the ones with the least deviation to the mean strength and elastic modulus, are highlighted.

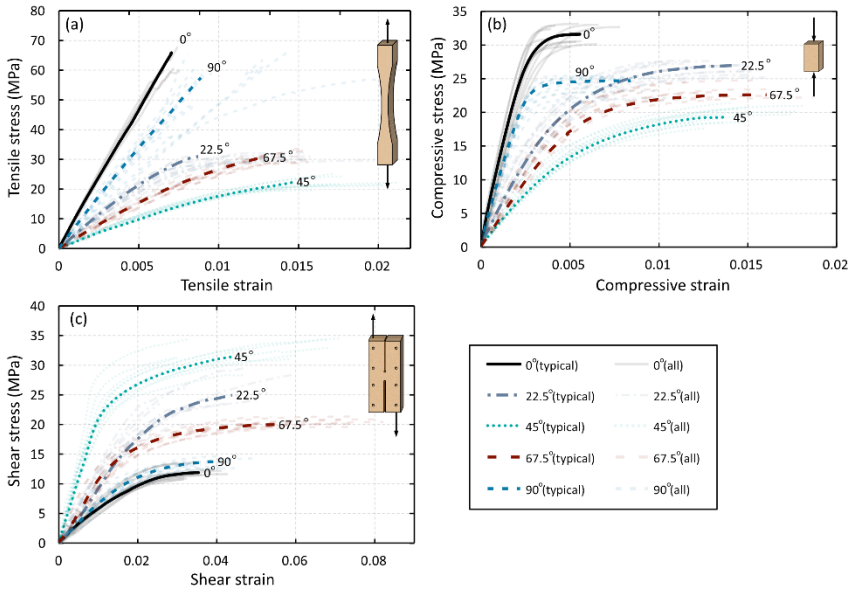

Figure 8: Stress-strain relationships of birch plywood specimens in (a) tension, (b) compression and (c) shear.

It is readily seen in Figure 8a-b that, the stress-strain curves in tension are practically linear elastic while those in compression exhibits elasto-plastic behavior, which is expected due to the nature of timber materials. For the

specimens tested in compression at 0° and 90°, distinct plastic plateau can be observed after yielding, while for the ones at 22.5°, 45° and 67.5°, hardening type plasticity is noticed.

As shown in Figure 8c, the shear stress grows linearly with the increase of the shear strain, followed by the nonlinearity before reaching the peak value. The nonlinear shear stress-strain relationships have been also reported by other investigations performed on beech plywood and maritime pine clear wood [46, 47].

The tensile and compressive strength and elastic modulus in relation to the loading angle to the face grain are displayed in Figure 9.

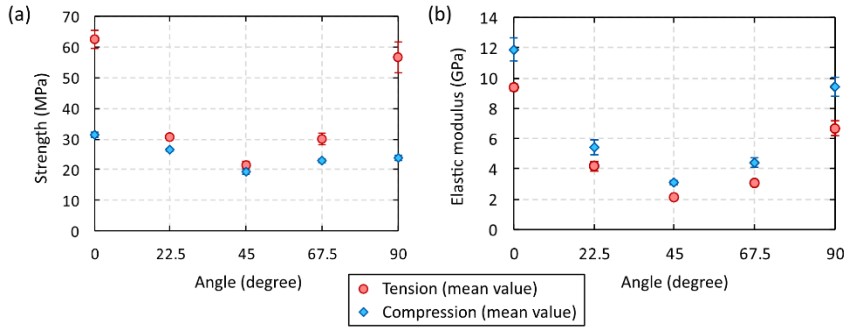

Figure 9: Tensile and compressive strength and modulus of birch plywood in relation to the load-to-face grain angle. The error bars denote a 95% confidence interval, based on one-sample t-tests.

Birch plywood exhibits the highest tensile strength at 0°, with mean tensile strength over 60 MPa. The tensile strength drops with the increase of the loading angle till 45°. Then, it increases gradually from 45° to 90°. The tensile strength at 45° is approximately 20 MPa, which is roughly one-third of that at 0°. The degree of angle-dependence of the compressive strength is lower than that of the tensile strength property, as shown in Figure 9a. Both tensile and compressive strength and elastic modulus at 90° are close to those at 0°, which can be explained by the cross lamination configuration of birch plywood.

The elastic modulus shows a similar tendency to the strength properties; but the angle-dependence is more noticeable. Moreover, it is observed that the elastic modulus derived from the compressive tests is

slightly higher than that from the tensile tests. Theoretically, the tensile and compressive elastic modulus should be identical. However, it is rarely the case in the laboratory tests. Different elastic modulus measured from the tensile and compressive tests were reported in previous studies for wood and plywood [48-50]. In this study, the compressive specimens were partially constrained due to the contact between the steel plates and the end surfaces of birch plywood during the loading. It is likely that this constraint might overrate the elastic modulus. On the other hand, there was no constraint in the middle part of the tensile specimen with the constant cross-sectional area. Thus, the elastic modulus derived from the tensile tests is considered to be more representative.

It is well-known that, for clear wood, the tensile strength parallel to the grain is higher than the compressive strength parallel to the grain. The opposite applies to structural timber. This is due to that, in structural timber, the existence of the growth irregularities, e.g., knots and grain deviation, etc., are inevitable. The tensile properties are more sensitive to these imperfections. Besides, tensile properties show volume effect due to the brittle fracture behavior [51]. As indicated in Figure 9a, birch plywood possesses higher tensile strength than compressive strength, which is the feature of clear wood. This observation is expected since the imperfections are redistributed in birch plywood.

The shear strength and modulus in relation to the loading angle to the face grain are presented in Figure 10.

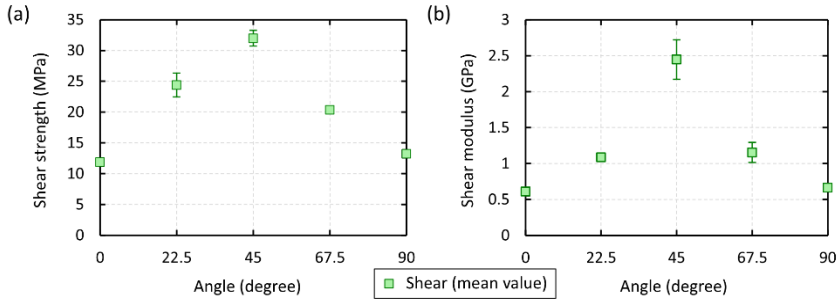

Figure 10: Shear strength and modulus of birch plywood in relation to the load-to-face grain angle. The error bars denote a 95% confidence interval, based on one-sample t-tests.

The angle dependence of the shear properties is the opposite of the tensile and compressive ones. This phenomenon can be explained with the help of the stress transformation model illustrated in Eq. 4 and Figure 5 in Section 2.2.2. When the tensile or compressive specimens were loaded in off-axis directions (i.e., there is an angle θ ($0° < \theta < 90°$) between the loading axis and the face grain angle), the on-axis shear stress (τ_{xy}) was activated and was the highest at 45°. The influence of the shear stress was dominant because the on-axis shear strength is much lower than the on-axis tensile or compressive strength (see Figure 9a and 10a).

Similarly, when the shear specimens were loaded in off-axis directions, the on-axis tensile and compressive strengths were involved and was the highest at 45°. The 'negative' influence of the shear stress was minimized at 45°, resulting in the highest off-axis shear strength at 45°.

It should be noted that, when comparing birch plywood with other commonly used structural timber elements, e.g., structural lumber or glulam, etc., the lowest tensile or compressive strength of birch plywood at 45° is more or less the same as the highest tensile or compressive strength of these timber elements in their longitudinal direction. The lowest panel shear strength of birch plywood at 0° and 90°, is remarkably higher than the shear strength of timber elements made of softwood [52]. Consequently, the outstanding mechanical properties of birch plywood make it promising to be applied for structural usage.

3.1.2. Predictions of off-axis strength

See the off-axis strength prediction results in Figure 11.

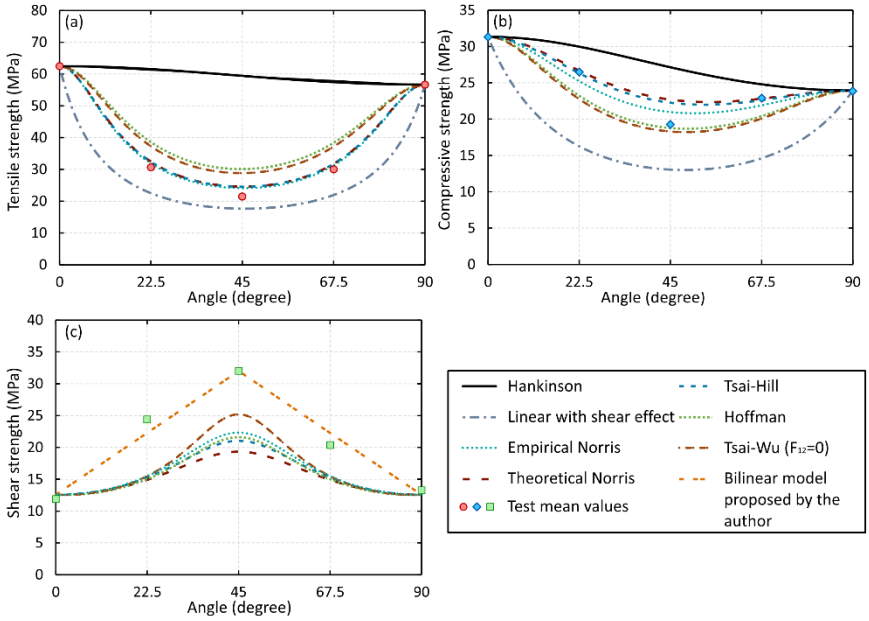

Figure 11: Comparison between the predicted strength properties and the test data.

To quantify the closeness of the predicted strengths to the test data, statistical analyses were performed by comparing the root mean square error ($RMSE$) of each failure criterion. $RMSE$ is expressed in Eq. 25.

$$RMSE = \sqrt{\frac{1}{5} \cdot \sum_{\theta} \left(f_{\theta,exp} - f_{\theta,pre}\right)^2} \quad (\theta = 0°, 22.5°, \dots, 90°), \tag{25}$$

where $f_{\theta,exp}$ and $f_{\theta,pre}$ are the strength obtained from the experiments and the predictions at an angle θ to the face grain, respectively. The failure criterion with the minimum $RMSE$ is considered as the one that fits the best to the test data. See the $RMSE$ results of each failure criterion in Table 7. The ones with the minimum $RMSE$ for each type of strength property were underlined.

Table 7: $RMSE$ values of each failure criterion. (unit: MPa)

Failure criterion	Tension	Compression	Shear
Hankinson	25.11	3.89	-
Linear with shear effect	5.39	6.56	-
Empirical Norris	1.39	1.05	6.27
Theoretical Norris	1.79	1.50	7.49
Tsai-Hill	1.75	1.31	6.78
Hoffman	6.45	1.88	6.70
Tsai-Wu (F_{12}=0)	5.47	2.18	5.47
Bilinear	-	-	1.34

As noticed in Figure 11a and 11b, the Hankinson's failure curve varies between the strengths at 0° and 90°, considerably above the test data. On the contrary, the other employed linear failure criterion is rather conservative. Both of them are not applicable for predicting the strength of birch plywood.

The quadratic failure criteria show better performance than the linear ones. In particular, the empirical Norris failure criterion gives the closest prediction to the tested tensile and compressive data, followed by Tsai-Hill and theoretical Norris failure criteria.

It is shown in Figure 11c and Table 7 that, all the criteria introduced in Table 2 underrate the panel shear strengths of birch plywood. Thus, one bilinear model is proposed by the author that linearly links the shear strengths at 0°, 45° and 90°, with much lower $RMSE$ than the others.

F_{12} would affect the predicted results, to some extent. However, the Tsai-Wu failure criterion is neither competitive to the empirical Norris failure criterion in tension and compression, nor to the bilinear model in panel shear.

In conclusion, the empirical Norris failure criterion is recommended in applications where the birch plywood is mainly subjected to tensile or compressive stresses. On the other hand, the bilinear model is suggested when the panel shear stress is dominant in the birch plywood plate.

3.1.3. Predictions of off-axis elastic properties

The elastic modulus prediction was compared to the experimental elastic modulus from the tensile tests since the results are more representative as mentioned before in Section 3.1.1.

The predicted results in comparison to the experimental data are presented in Figure 12.

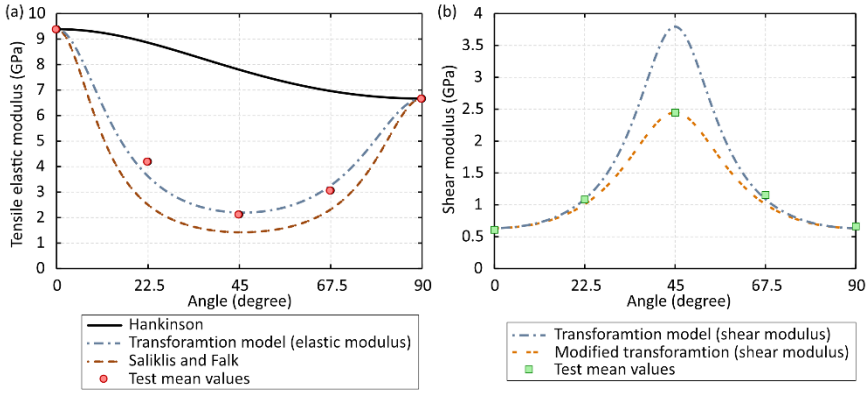

Figure 12: Comparison between the predicted elastic properties and the test data.

It is evident that the transformation model predicts the elastic modulus quite well but overestimates the shear modulus. It is worth mentioning that, the Poisson's ratio ν_{xy}, as one of the parameters in the transformation model, was derived instead of being tested. Sensitivity analysis has been performed in Paper I to study its influence on the elastic property prediction. It is found that its effect on the off-axis elastic modulus is negligible. Moreover, ν_{xy} would influence the shear modulus prediction. Nevertheless, the modified transformation model is always the better one.

3.2. Edgewise bending properties

3.2.1. Factor I: face grain angle

3.2.1.1. Experimental results

The influence of the face grain angle on the edgewise bending properties of birch plywood can be revealed from the experimental results of test series No. 01-05. The mean experimental ultimate moment capacity $M_{u,exp}$, the edgewise bending strength f_b and the elastic bending modulus MOE_b are listed in Table 8.

Table 8: Mean experimental results of the test series No. 01-05

Test series No.	$M_{u,exp}$ (Nm)	f_b (MPa)	MOE_b (GPa)
01	559.4 (4.8)	65.1 (4.7)	10.6 (6.9)
02	354.4 (3.7)	41.5 (3.5)	4.4 (4.0)
03	264.0 (4.6)	31.0 (4.5)	2.4 (4.7)
04	311.0 (2.4)	36.6 (2.7)	3.4 (5.9)
05	417.3 (7.1)	48.7 (7.5)	7.3 (8.8)

Note: the numbers within parentheses indicate the COV values.

As expected, when the face grain angle varies from 0° to 90°, the bending properties exhibit a similar tendency to the tensile and compressive properties; birch plywood specimens possess the highest moment capacity and the elastic bending modulus at 0° and both the lowest at 45°.

3.2.1.2. Prediction results

The analytical and numerical ultimate moment capacities ($M_{u,anl}$ and $M_{u,num}$) at five different angles to the face grain were compared with the experimental ones ($M_{u,exp}$), as shown in Figure 13.

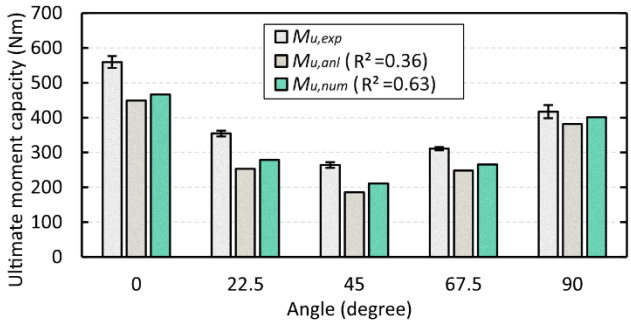

Figure 13: Comparison between the predicted and tested ultimate moment capacities. The error bars denote a 95% confidence interval, based on one-sample t-tests.

It is noticed in Figure 13 that both $M_{u,anl}$ and $M_{u,num}$ underestimate the ultimate moment capacities at all the five angles to the face grain, which may be attributed to the conservative failure definition. Tensile strength is determined by the uniaxial tensile test where the tensile stress is nearly uniform on the cross section. The weakest fiber governs the tensile strength due to the weakest link theory [53]. In edgewise bending, only the extreme fiber in the bottom is subjected to the highest tensile stress. This smaller part has a higher probability to be defect-free, i.e., not the weakest link in the material. Hence, it may be reasonable to check the average stress of a certain part of the cross-sectional area from the bottom. See Figure 14 for the illustration of the different failure definitions. The influence of the defined area on the prediction of the ultimate moment capacities is shown in Figure 15.

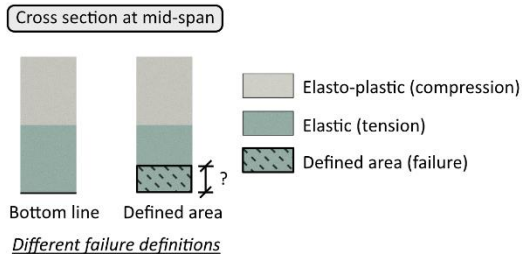

Figure 14: Illustration of different failure definitions.

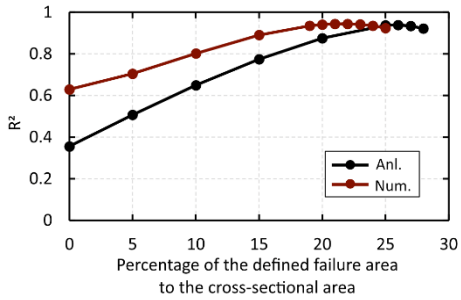

Figure 15: Parametric analysis of the percentage of the defined failure area to the cross-sectional area.

As shown in Figure 15, R square reaches the highest value, i.e., predicting the closest results to $M_{u,exp}$, when the defined failure area is around 20-25% of the cross-sectional area.

3.2.2. Factor II: size

In order to study the size effect on the edgewise bending properties, birch plywood beams with the nominal depths of 20 mm and 50 mm (test series No. 01-05 and No. 10-14) were firstly tested in the time sequence. It is found that the size effect on the edgewise bending strength is noticeable on the specimens at 0° and 90° but nearly negligible at 22.5°, 45°, and 67.5° (see Figure 16). Therefore, the specimens with the nominal depth of 40 mm and 30 mm (test series No. 06-09), were loaded at 0° and 90°, to further study the size effect between 20 mm and 50 mm.

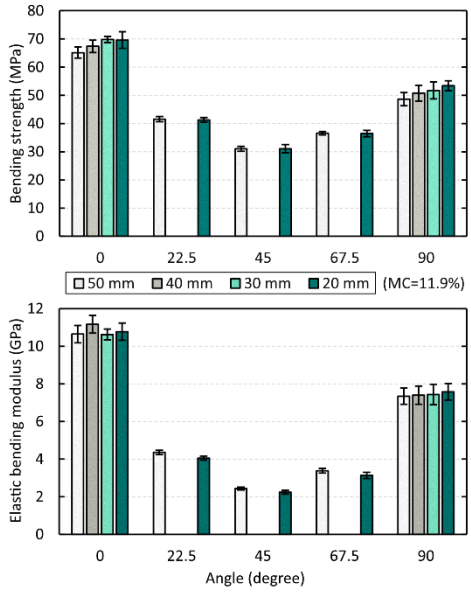

Figure 16: Edgewise bending strength and elastic bending modulus of beams with different sizes, corresponding to test series No. 01-14. The error bars denote a 95% confidence interval, based on one-sample t-tests.

The discrepancy mentioned above can be explained by their different failure characteristics. See the load-LVDT displacement curves at the five angles to the face grain in Figure 17.

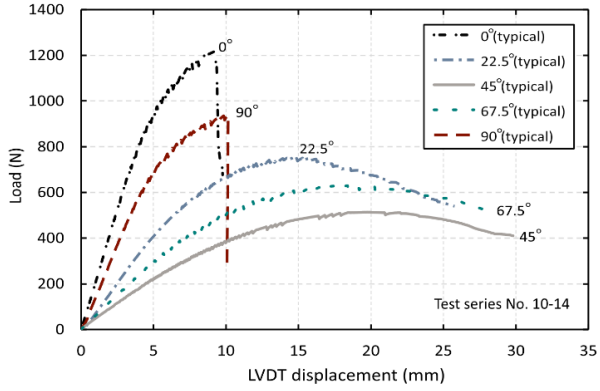

Figure 17: Load-LVDT displacement curves (test series No. 10-14)

For the birch plywood beams at 0° and 90°, force dropped dramatically once reaching the peak. While for the beams at 22.5°, 45°, and 67.5°, the post-peak behavior is significantly different that force decreased gradually instead. Consequently, at 0° and 90°, birch plywood beams with the brittle failure mode are more dependent on the stressed volume. Moreover, the size effect on the elastic modulus is not noticeable.

3.2.3. Factor III: moisture content

As noticed in Table 5, birch plywood beams were tested at three MC levels, i.e., 7.2%, 11.9% and 21.8%, with the constant nominal depth of 20 mm (test series No. 10-24). See Figure 18 for the test results.

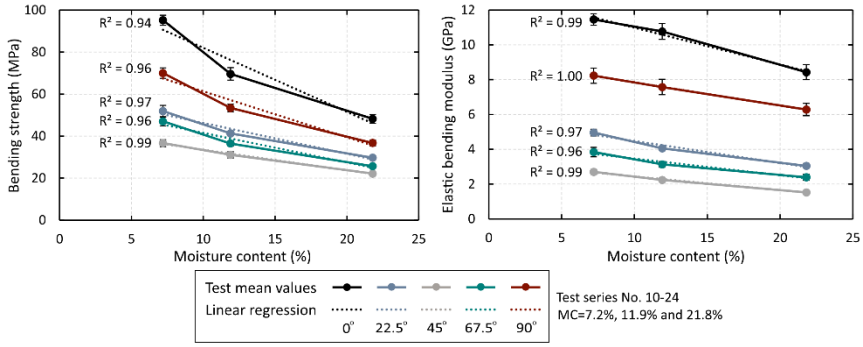

Figure 18: Edgewise bending strength and elastic modulus in relation to the moisture contents, corresponding to test series No. 10-24. The error bars denote a 95% confidence interval, based on one-sample t-tests.

Both the bending strength and elastic bending modulus decrease when the moisture content rises up in the hygroscopic range. The linear regression models generalize the moisture effects fairly well with the lowest R square value of 0.94.

3.2.4. Bending strength–elastic bending modulus relationships

The bending strength and elastic bending modulus of each specimen from each test series are plotted in Figure 19.

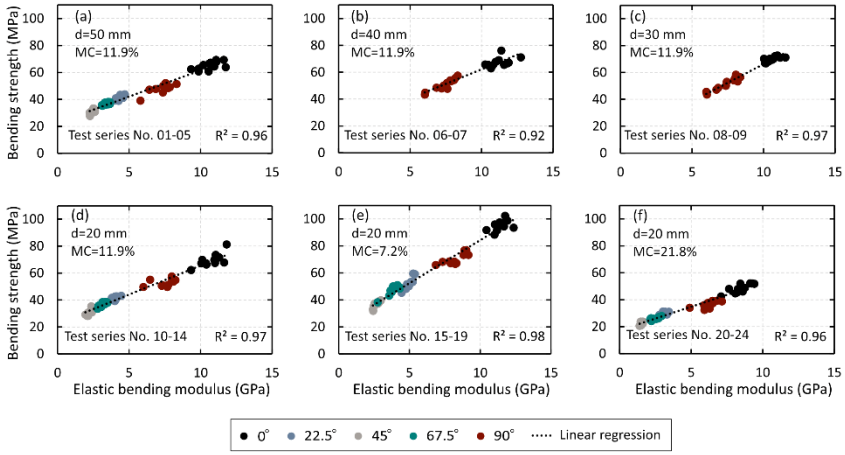

Figure 19: Relationships between edgewise bending strength and elastic bending modulus.

The relationship between strength and modulus can be well expressed by a linear function (see the black dashed line in Figure 19). The strong relationships confirm the feasibility of assessing the edgewise bending strength of birch plywood by detecting its elastic modulus non-destructively.

4. Conclusions and future work

In this thesis, the in-plane mechanical properties of birch plywood at varying angles to the face grain are characterized experimentally and successfully predicted by analytical and numerical models. The influence of size and moisture content on the edgewise bending properties is investigated. Knowledge obtained from the thesis work is crucial for the practical design of birch plywood plates in timber connections.

The experimental results indicate that birch plywood possesses satisfying mechanical properties in all in-plane directions, thereby promising for structural uses. To be more specific, even the lowest tensile and compressive strengths at 45° are around 20 MPa; the lowest edgewise bending strength at 45° is over 30 MPa and the lowest panel shear strength at 0° and 90° is over 10 MPa. All these strength values are similar to or higher than the highest strengths of other commonly used timber-based materials when loaded in the grain direction.

Regarding the prediction models, the empirical Norris failure criterion is recommended for the tensile and compressive strength predictions while the bilinear model is the best for shear strength predictions. The edgewise bending strength prediction relies on the tensile and compressive stress-strain relationships as input and is highly dependent on the failure definitions in both analytical and numerical models. The transformation model shows the highest closeness to the tested elastic modulus while the modified one predicts the shear modulus better.

A size effect is observable at 0° and 90° but not at other angles in edgewise bending, owing to the different failure mechanisms. Linear functions generalize the moisture effect fairly well. Strong relationships between edgewise bending strength and elastic modulus imply the feasibility to derive the angle-dependent bending strength by detecting its elastic modulus non-destructively.

Having the comprehensive experimental database established, the next step is to investigate the structural behavior of birch plywood as gusset plates in timber connections. Particular interests comprise glued connections between birch plywood and other timber elements, e.g., spruce glulam. Studies about such wood-adhesive bonding performance are planned as the future work.

References

[1] T. Sellers, Plywood and adhesive technology, Marcel Dekker Inc, New York (1985).

[2] M. McDowall, L.M. Punton, Structural Plywood & LVL Design Manual, Engineering Wood Product Association of Australia (2007). http://www.5startimbers.com.au/downloads/Structural_Ply_LVL_Design_Manual_P1.pdf.

[3] M. Hughes, Plywood and other veneer-based products, In M.P. Ansell, editor (Ed.), Wood composites, Woodhead Publishing (2015) pp. 69-89. https://doi.org/10.1016/B978-1-78242-454-3.00004-4.

[4] A.W. Boehner, M.S.H. Bhuiyan, Wood: Structural Panel Processes, Reference Module in Materials Science and Materials Engineering (2016). https://doi.org/10.1016/B978-0-12-803581-8.02224-4.

[5] A. Sotayo, D. Bradley, M. Bather, P. Sareh, M. Oudjene, I. El-Houjeyri, A.M. Harte, S. Mehra, C. O'Ceallaigh, P. Haller, S. Namari, A. Makradi, S. Belouettar, L. Bouhala, F. Deneufbourg, Z. Guan, Review of state of the art of dowel laminated timber members and densified wood materials as sustainable engineered wood products for construction and building applications, Developments in the Built Environment 1 (2020) 100004. https://doi.org/10.1016/j.dibe.2019.100004.

[6] H.R. Milner, A.C. Woodard, 8 - Sustainability of engineered wood products, In: J.M. Khatib, editor (Ed.), Sustainability of Construction Materials (Second Edition), Woodhead Publishing, (2016) pp. 159–180. https://doi.org/10.1016/B978-0-08-100370-1.00008-1.

[7] Finnish Forest Industries Federation. Handbook of Finnish Plywood (2002). https://www.koskisen.com/file/handbook-of-finnish-plywood/.

[8] J.M. Dinwoodie, Timber: its nature and behaviour, CRC Press (2000).

[9] 2 - Wood as bio-based building material, In: D. Jones, C. Brischke, editor(s) (Eds.), Performance of Bio-based Building Materials, Woodhead Publishing (2017) pp. 21-96. https://doi.org/10.1016/B978-0-08-100982-6.00002-1.

[10] K.I. Crews, 12 - Nonconventional timber construction, In: K.A. Harries, B. Sharma, editor(s) (Eds.), Nonconventional and Vernacular Construction Materials, Woodhead Publishing (2016) pp. 335–363. https://doi.org/10.1016/B978-0-08-100038-0.00012-3.

[11] Design of wood aircraft structures, U.S. Govt., Print. Off (1944). https://doi.org/10.5479/sil.1018746.39088017549809.

[12] G. Säfwe, R. Wåhlander, Monteringsstudie av träfackverk med förband av björkplywood, Bachelor thesis, KTH Royal Institute of Technology, Stockholm, Sweden (2021).

[13] Plywood applications in timber connections. https://www.linkedin.com/company/forum-holzbau/posts/?feedView=all. (Accessed 27 October 2022).

[14] R. Crocetti, Large-span timber structures, In Proceedings of the World Congress on Civil, Structural, and Environmental Engineering, Mar 30-31, Prague, Czech Republic, (2016), pp. 1-23. https://avestia.com/CSEE2016_Proceedings/files/paper/ICSENM/124.pdf.

[15] R.B. Abrahamsen, K.A. Malo, Structural design and assembly of treet – a 14-storey timber residential building in Norway, In: Proceedings of the world conference on timber engineering, Aug 10-14, Quebec City, Canada, (2014).

[16] M. Xu, Z. Cui, F, Lam, Q. Xu, Z. Chen, Splitting load-carrying capacity of steel-to-laminated bamboo dowel connections with slotted-in steel plates, Journal of Building Engineering 42 (2021) 102805. https://doi.org/10.1016/j.jobe.2021.102805.

[17] C. Erchinger, A. Frangi, M. Fontana, Fire design of steel-to-timber dowelled connections, Engineering Structures 32(2) (2010) 580-589. https://doi.org/10.1016/j.engstruct.2009.11.004.

[18] C. Sandhaas, Mechanical behaviour of timber joints with slotted-in steel plates, Doctoral dissertation, Delft University of Technology, Delft, The Netherlands (2012).

[19] D.J.J. del Coz, P.G. Nieto, A.L. Martínez-Luengas, F.S. Domínguez, J.D. Hernández, Non-linear numerical analysis of plywood board timber connections by DOE-FEM and full-scale experimental validation, Engineering Structures 49 (2013) 76–90. https://doi.org/10.1016/j.engstruct.2012.11.003.

[20] E. Furuheim, P.M. Nesse, R. Crocetti, R. Tomasi, D. Pasca, H. Liven, R. Abrahamsen, Connections for post and beam glulam structures using birch plywood plates and screws, In: Proceedings of the world conference on timber engineering, Aug 9-12, Santiago, Chile, (2021).

[21] J. Hynynen, P. Niemistö, A. Viherä-Aarnio, A. Brunner, S. Hein, P. Velling, Silviculture of birch (Betula pendula Roth and Betula pubescens Ehrh.) in northern Europe, Forestry 83 (1) (2010) 103–119. https://doi.org/10.1093/forestry/cpp035.

[22] J.B. Boutelje, R. Rydell, Träfakta: 44 träslag i ord och bild (1995). http://www.diva-portal.org/smash/record.jsf?pid=diva2%3A1073763&dswid=-8161.

[23] H. Holmberg, D. Sandberg, Structure and properties of Scandinavian Timber, HoS Grenarna AB (1997). https://www.diva-portal.org/smash/get/diva2:995224/FULLTEXT01.pdf.

[24] C.B. Norris, Strength of orthotropic materials subjected to combined stress, U.S. Department of Agriculture, Forest Products Laboratory, Forest Service (1950).

[25] H. Bier, Strength properties of pinus radiata plywood at angles to face grain, New Zealand Journal of Forestry Science 14 (3) (1984) 349–367.

[26] V.J. Popovska, B. Iliev, G. Zlateski, Impact of veneer layouts on plywood tensile strength, Drvna industrija 68 (2) (2017) 153–161. https://doi.org/10.5552/drind.2017.1634.

[27] R.Z. Yang, Y. Xiao, F. Lam, Failure analysis of typical glubam with bidirectional fibers by off-axis tension tests, Construction and Building Materials 58 (2014) 9–15. https://doi.org/10.1016/j.conbuildmat.2014.02.014.

[28] BS EN 322: 1993, Wood-based panels – Determination of moisture content, European Committee for Standardization (CEN) (1993).

[29] ASTM D3500-14, Standard Test Methods for Structural Panels in Tension, ASTM International (2014).

[30] ASTM D3501-05a, Standard Test Methods for Structural Panels in Compression, ASTM International (2018).

[31] EN 789: 2004, Timber structures - Test methods - Determination of mechanical properties of wood based panels, European Committee for Standardization (CEN) (2004).

[32] ASTM D1037-12, Standard Test Methods for Evaluating Properties of Wood-Base Fiber and Particle Panel Materials, ASTM International (2012).

[33] ASTM D2719-19, Standard Test Methods for Wood Structural Panels in Shear Through-the-Thickness, ASTM International (2019).

[34] R.L. Hankinson, Investigation of crushing strength of spruce at varying angles of grain, Air service information circular 3(259) (1921) 130.

[35] Forest Products Laboratory (U.S.), Design of wood aircraft structures, U.S. Govt., Print. Off (1944). 10.5479/sil.1018746.39088017549809.

[36] R. Hill. A theory of the yielding and plastic flow of anisotropic metals, Proceedings of the Royal Society of London 193(1033) (1948) 281-97. https://doi.org/10.1098/rspa.1948.0045.

[37] V.D. Azzi, S.W. Tsai. Anisotropic strength of composites, Experimental mechanics 5(9) (1965) 283-8. https://doi.org/10.1007/BF02326292.

[38] O. Hoffman, The brittle strength of orthotropic materials, Journal of Composite Materials 1(2) (1967) 200-6. https://doi.org/10.1177/002199836700100210.

[39] S.W. Tsai, E.M. Wu, A general theory of strength for anisotropic materials, Journal of composite materials 5(1) (1971) 58-80. https://doi.org/10.1177/002199837100500106.

[40] J. Bodig, B.A. Jayne, Mechanics of Wood and Wood Composites, New York: Van Nostrand Reinhold (1982).

[41] R.M. Jones, Mechanics of Composite Materials (2nd ed.), CRC Press (1999). https://doi.org/10.1201/9781498711067.

[42] E.P. Saliklis, R.H. Falk, Correlating off-axis tension tests to shear modulus of wood-based panels, Journal of structural engineering 126(5) (2000) 621-5. https://doi.org/10.1061/(ASCE)0733-9445(2000)126:5(621).

[43] H. Yoshihara, Influence of the specimen depth to length ratio and lamination construction on Young's modulus and in-plane shear modulus of plywood measured by flexural vibration, BioResources 7(1) (2012) 1337-51.

[44] Y. Wang, T. Wang, R. Crocetti, M. Wålinder, Experimental investigation on mechanical properties of acetylated birch plywood and its angle-dependence, Construction and Building Materials 344 (2022) 128277. https://doi.org/10.1016/j.conbuildmat.2022.128277.

[45] P.F. Pai, A new look at shear correction factors and warping functions of anisotropic laminates, International Journal of Solids and Structures 32(16) (1995) 2295-2313. https://doi.org/10.1016/0020-7683(94)00258-X.

[46] J. Viguier, B. Marcon, J.C. Butaud, L. Denaud, R. Collet, Panel Shear of Plywood in Structural Sizes-Assessment Improvement Using Digital Image Correlation, Experimental Techniques 45(2) (2021) 195-206. https://doi.org/10.1007/s40799-020-00430-4.

[47] J.C. Xavier, N.M. Garrido, M. Oliveira, J.L. Morais, P.P. Camanho, F. Pierron, A comparison between the Iosipescu and off-axis shear test methods for the characterization of Pinus Pinaster Ait, Composites Part A: Applied Science and Manufacturing 35(7-8) (2004) 827-40. https://doi.org/10.1016/j.compositesa.2004.01.013.

[48] N. Baldassino, P. Zanon, R. Zanuttini, Determining mechanical properties and main characteristic values of Poplar plywood by medium-sized test pieces, Materials and Structures 31(1) (1998) 64-7. https://doi.org/10.1007/BF02486416.

[49] F. Arriaga-Martitegui, F. Peraza-Sánchez, L. García-Esteban, Characteristic values of the mechanical properties of radiata pine plywood and the derivation of basic values of the layers for a calculation method, Biosystems Engineering 99(2) (2008) 256-66. https://doi.org/10.1016/j.biosystemseng.2007.10.004.

[50] U. Dackermann, R. Elsener, J. Li, K. Crews, A comparative study of using static and ultrasonic material testing methods to determine the anisotropic material properties of wood, Construction and Building Materials 102 (2016) 963-76. https://doi.org/10.1016/j.conbuildmat.2015.07.195.

[51] H.J. Blaß, C. Sandhaas, Timber engineering-principles for design, KIT Scientific Publishing (2017).

[52] R. Crocetti, M. Johansson, H. Johnsson, R. Kliger, A. Mårtensson, B. Norlin, A. Pousette, S. Thelandersson, Design of Timber Structures, Stockholm: Swedish Wood (2011).

[53] W. Weibull, A Statistical Theory of the Strength of Materials, in: Stockholm (1939).